

Christophe Daniel
Ian W. Hamley
Manfred Wilhelm
Withawat Mingvanish

Non-linear rheology of a face-centred cubic phase in a diblock copolymer gel

Received: 31 May 2000
Accepted: 21 August 2000

C. Daniel · I. W. Hamley (✉)
School of Chemistry, University of Leeds
LS2 9JT, UK
e-mail: I.W.Hamley@chem.leeds.ac.uk

M. Wilhelm
Max-Planck-Institut für Polymerforschung
Postfach 3148, 55021 Mainz, Germany

W. Mingvanish
Department of Chemistry
University of Manchester
Manchester M13 9PL, UK

Abstract The viscoelastic behaviour of a poly(oxyethylene)-poly(oxybutylene) diblock copolymer in aqueous solution forming a face-centred cubic (fcc) micellar phase has been investigated using oscillatory shear rheometry. With increasing strain amplitude, the micellar solution was observed to undergo a transition from linear to non-linear behaviour, characterized by strong shear thinning. The non-linear behaviour observed in the stress response was analyzed by Fourier transformation of the waveform. Fourier analysis revealed that the high harmonic contributions to the shear stress response increased with strain amplitude and up to the 81st harmonic was observed for very large amplitudes. The onset of non-linear response as defined from the

dependence of isochronal dynamic shear moduli on strain amplitude was found to be in good agreement with that defined by the appearance of a higher harmonic in the stress waveform. The amplitudes of the harmonic coefficients are compared to the predictions of a model for the nonlinear rheological response of a lyotropic cubic mesophase based on the stress response to a periodic lattice potential (Jones and McLeish 1995). It is found that the model is able to account for qualitative trends in the data such as the development of finite higher harmonics with increasing strain, but it does not describe the full frequency and strain dependence of these coefficients.

Key words Block copolymer · Micelle · Non-linear rheology

Introduction

Concentrated solutions of block copolymers can form various liquid crystalline phases characterized by a finite yield stress. Depending on the copolymer structure or the concentration and the temperature of the solution, a variety of ordered phases can be obtained such as cubic, hexagonal or lamellar structures. The phase behaviour and structure of block copolymer gels have been widely studied and this work has been recently reviewed (Hamley 1998).

Of particular interest is the viscoelastic behaviour of block copolymer gels and the effect of shearing on their structure and their rheological properties. Due to their numerous commercial applications, aqueous solutions

of poly(oxyethylene)-poly(oxypropylene)-poly(oxyethylene) ($E_m P_n E_m$ where m and n denote the number of repeat units) triblock copolymers have probably been the most extensively studied system. For example, a complex viscoelastic behaviour was observed with $E_{21} P_{47} E_{21}$ Pluronic solutions where two gel structures referred as “hard gel” and “soft gel” were identified (Hvidt et al. 1994). The former structure was characterised by a dynamic shear elastic modulus $G' > 10^4$ Pa while the latter structure displayed a dynamic shear modulus about three orders of magnitude smaller. The formation of the so-called “hard” gel was associated with the development of a cubic arrangements of the micelles (Mortensen 1992; Almgren et al. 1995). In poly(oxyethylene)-poly(oxybutylene) (EB) diblock solu-

tions, “hard” gels were also shown to correspond to cubic micellar structures, either face-centered cubic (fcc) or body-centred cubic (bcc) (Pople et al. 1997). On the other hand soft gels often correspond to lamellar or hexagonal structures (Yu et al. 1998; Pople et al. 1999).

Cubic arrangements of micelles can be aligned either by steady shear or large amplitude oscillatory shear (LAOS) and a large body of work has focused on the effects of shear on the orientation of block copolymer gels (Mortensen et al. 1992; McConnell et al. 1995; Molino et al. 1998; Hamley et al. 1998). In all these studies, small angle scattering experiments were performed on gels under flow. However, the non-linear rheology resulting from LAOS applied to micellar gels has received less attention and this is the focus of the present paper.

An investigation of the non-linear viscoelastic behavior of the bcc micellar phase formed by the diblock copolymer $E_{86}B_{10}$ in aqueous solution showed that slip-stick mechanisms of flow characterized by lozenge-shaped Lissajous patterns of stress versus strain occurred at large shear strain amplitudes (Hamley et al. 1998). The macroscopic orientation of the sample was associated with the onset of the slip-stick mechanism in the cubic lattice. This slip-stick mechanism observed at large strains was consistent with the model developed by Doi et al. (1993) for the rheology of block copolymers forming a periodic mesophase. This theory predicts the onset of nonlinear rheological behaviour due to the relative slippage of lattice planes. Non-linear flows in ordered micellar mesophases formed in solutions of poly(styrene)-poly(butadiene) (PS-PB) (Watanabe et al. 1982) and poly(styrene)-poly(isoprene)-poly(styrene) (PS-PI-PS) (Watanabe et al. 1997) block copolymers have been also examined in some detail. In these studies a transition from elastic to nonlinear response with lozenge-shaped Lissajous patterns was observed when increasing the strain amplitude. Furthermore, the non-linear stress response was decomposed as a Fourier series and it was found that for a given strain the non-linearity in the shear response decreased with increasing frequency.

The ordering of block copolymer micelles has strong analogies with that of colloidal latex particles that interact through repulsive pair potentials such as inverse power potentials or the Yukawa potential. Experiments and computer simulations on such systems indicate that if the interaction is short-range as for hard spheres, the system favours an fcc phase, whereas longer-range interactions among soft spheres lead to a bcc phase. The effect of shear on fcc arrays of colloidal particles (Ackerson and Pusey 1988; Ackerson 1990; Chen et al. 1994; Dux et al. 1996; Clarke et al. 1997) and bcc colloidal suspensions (Ackerson and Clark 1984) has been examined in detail, and the analogous behaviour of block copolymer solutions has frequently been com-

mented upon (McConnell et al. 1995; Berret et al. 1996; Molino et al. 1998; Leyh et al. 1998; Hamley et al. 1998a; Hamley 2000; Hamley et al. 2000).

In this paper we report on the non-linear rheology of an aqueous solution of the diblock copolymer $E_{96}B_{18}$ forming an fcc gel. The purpose of our investigation was to study the non-linear rheological response of a micellar structure at large strains and to investigate the effect of increasing the amplitude of oscillatory shear on this behaviour. We have used a recently introduced technique in which the non-linear response of the micellar solution is analysed using the so-called “high sensitivity Fourier-transform rheology” method (Wilhelm et al. 1998; Wilhelm et al. 1999).

When an oscillatory shear strain with a single frequency ω_0 is applied in the linear viscoelastic regime, the stress is also sinusoidal with the same frequency ω_0 . When the deformation is applied in the non-linear viscoelastic regime the stress response is no longer sinusoidal but can be represented as a Fourier series containing multiple harmonics (Wilhelm et al. 1998). This property has been used in the literature to investigate the non-linear behaviour of non-Newtonian fluids (Gamota et al. 1993; Reimers and Dealy 1996; Reimers and Dealy 1998) and ordered micellar structures subjected to LAOS (Watanabe et al. 1982; Watanabe et al. 1997). Recently this concept was extended and it was shown that Fourier analysis of the shear response in the non-linear regime can generate high order harmonics (Wilhelm et al. 1998; Wilhelm et al. 1999). In addition to enabling the determination of the onset of the non-linear response this method also permits a quantitative analysis of the effects of shear on the non-linear response.

A simple model for the rheological response of cubic phases formed by surfactants has been developed, that in addition to modelling the linear response makes predictions for the amplitudes of the harmonics in the non-linear stress response (Jones and McLeish 1995). The model is based on the elastic and viscous stresses acting on Maxwell-Voigt cells on a lattice. This lattice should have the symmetry of the cubic phase (for example, face-centered cubic in the case of our block copolymer surfactant micellar phase). Because there is no bulk relaxation in the Maxwell-Voigt model it predicts a solid-like response even at low frequencies, and thus the theory was extended to allow for a finite density of slip planes (Jones and McLeish 1995). A further development of the model accounted for the non-linear response resulting from the periodic lattice potential. A weak elastic force at the slip plane was introduced to account for this potential, further details being provided below. Although the model is rather restricted, in that it is developed in a “pseudolinear” approximation, it is the only model currently to make predictions for the amplitudes of the non-linear stress harmonics. Other

limitations of the theory include the neglect of effects such as local hydrodynamics and osmotic forces acting on micelles. We hope that the experimental results described herein will stimulate the development of a more complete theory that incorporates these effects.

In this report, preliminary results obtained with a fcc micellar gel are presented. At large strain amplitudes of oscillatory shear, strong shear thinning is observed. The Fourier analysis of the shear response showed that the non-linear contribution to the stress increases with strain amplitude and up to the 81st harmonic can be obtained. The first harmonic was found to vary with $\log(A)$, where A is the strain amplitude, for moderate strain amplitude, before reaching an asymptotic value. The Jones-McLeish theory for stress harmonics caused by a periodic lattice potential is found to qualitatively account for the monotonic decrease in the amplitude of successive harmonics, observed under conditions of fixed strain. The relative increase in the amplitude of the higher harmonic with increasing strain is also captured by the model, but it is not possible to quantitatively fit our experimental data. This points to the need to develop the model to account more realistically for the deformation of the micelles.

Experimental

A. Materials and sample preparation

The diblock copolymer $E_{96}B_{18}$ was prepared by sequential anionic polymerisation of ethylene oxide followed by 1,2-butylene oxide. The monofunctional initiator was 2(2-methoxyethoxy)ethanol activated by reaction with potassium metal (mole ratio OH/K \approx 5). Vacuum line and ampoule methods were used for the synthesis. ^{13}C NMR spectra gave a number-average molar mass, $\bar{M}_n = 5,500 \text{ g mol}^{-1}$ and gel permeation chromatography calibrated with poly(oxyethylene) standards indicated a narrow chain length distribution, i.e. $\bar{M}_w/\bar{M}_n = 1.03$ where \bar{M}_w is the weight average molar mass. Further details of the synthesis and copolymer characterization can be found elsewhere (Mingvanish et al. 2000).

The diblock copolymer gel investigated in this report had a concentration of 15 wt% in water, and was prepared by mixing at 60–70 °C until dissolution was complete.

B. Techniques

Rheology experiments were performed with a Rheometrics ARES rheometer by applying oscillatory strains to the gel. A cone-and-plate geometry with a 25 mm diameter and a 0.1 rad cone angle was used for all the

measurements. Because all measurements were conducted at $T = 22 \text{ }^\circ\text{C}$, and the time per measurement was small ($t < 1 \text{ hr}$), evaporation was negligible for the samples studied. Furthermore, in the cone-and-plate geometry the contact of sample with the air is small. Voltage signals corresponding to the input sinusoidal strain and the output force transducer signal (proportional to stress) were digitized on a LeCroy 9304C Oscilloscope. Approximately 20 cycles of the fundamental frequency were acquired and the shear stress was analyzed using the Fourier transformation algorithm incorporated in the oscilloscope, and off-line using the program Origin 3.5 (Microcal Software Inc.).

Small angle x-ray scattering experiments were performed at the Synchrotron Radiation Source, Daresbury Laboratory, U.K. Beam-line 2.1 was used with an x-ray wavelength $\lambda = 1.5 \text{ \AA}$. The SAXS patterns were recorded on a multiwire gas-filled area detector located at 3 m from the sample. A scattering pattern from an oriented specimen of wet collagen (rat tail tendon) was used for the calibration of the q scale range, ($q = 4\pi \sin \theta/\lambda$, where the scattering angle is defined as 2θ). All experiments were conducted at room temperature.

Results and discussion

Figure 1 shows the profile of the scattered intensity versus q for a 15 wt% aqueous gel of $E_{96}B_{18}$ at 20 °C, obtained by radial integration of a 2D SAXS pattern. We observe a series of peaks in the positional ratio $1:(8/3)^{1/2}:(11/3)^{1/2}$ with a first-order reflection located at

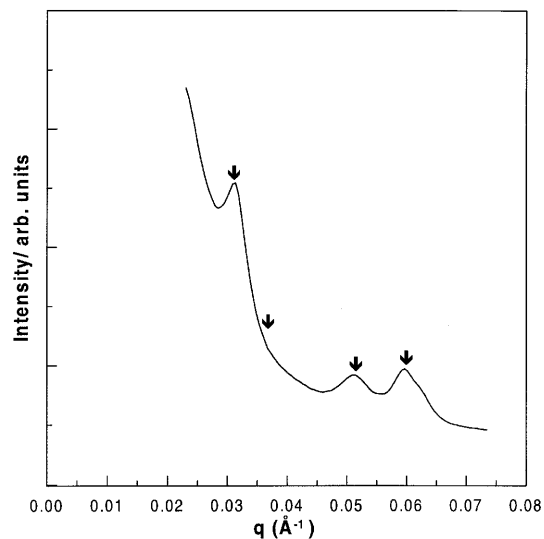


Fig. 1 Profile of intensity versus wavenumber for an aqueous gel containing 15 wt% $E_{96}B_{18}$ at 20 °C, obtained by radial integration of a 2D SAXS pattern. The arrows indicate the position of expected reflections for an fcc structure

$q^* = 0.031 \text{ \AA}^{-1}$. This sequence of peaks is consistent with the 111, 220, and 311 reflections of an fcc structure ($Fm\bar{3}m$ symmetry) with a lattice parameter $a = 351 \text{ \AA}$ and a distance between nearest neighbours $d = 248 \text{ \AA}$. The absence of the 200 reflections (missing peak at $(4/3)^{1/2}q^*$) is due to the orientation of the gel that occurred during the sample loading, as discussed elsewhere (Hamley et al. 1999).

The extent of the linear viscoelastic regime for the gel was determined by performing a “strain sweep” at a fixed frequency $\omega_0 = 1 \text{ Hz}$ and plotting the variation of G' and G'' as a function of the strain amplitude, as shown in Fig. 2a. This indicates a linear behaviour up to approximately 0.5% strain where G'' starts to increase. Of course, in the non-linear regime, G' and G'' are not defined correctly by the rheometer software. In this

region, the stress should be represented as a Fourier series with non-zero higher harmonics (see Eq. (1)). A frequency sweep performed in the linear viscoelastic regime is shown in Fig. 2b. This shows that G' is essentially independent of frequency in the range examined and its value $G' > 10^4 \text{ Pa}$ is consistent with a “hard gel”, cubic, structure (Hvidt et al. 1995). The frequency dependence of the dynamic moduli indicate that the crossover of G' and G'' that defines the characteristic relaxation time will occur for $\omega_0 > 20 \text{ Hz}$, i.e. $t_0 < 0.05 \text{ s}$. Thus at a probe frequency $\omega = 1 \text{ Hz}$, the rheological response is dominated by the mesophase structure (here a cubic lattice) rather than molecular relaxation processes.

In Fig. 3, the stress and strain wave forms obtained at a fixed frequency ($\omega_0 = 1 \text{ Hz}$) but different strain amplitudes are plotted on the left-hand side while Lissajous figures of the stress (force) against strain are shown on the right-hand side. For a strain amplitude of $A = 1\%$ (bottom), the stress wave is sinusoidal and in phase with the strain wave and the Lissajous pattern is a line. Care was taken to record steady state waveforms, which developed several cycles after the startup of shear. For this deformation, the sample therefore behaves as a pure elastic solid. For a larger amplitude $A = 5\%$, the sample exhibits viscoelastic behaviour and the stress wave is out of phase with the input strain. The Lissajous pattern is elliptical with a small kink at the upper right and lower left extremities indicating a small non-linear effect. When the strain is increased to $A = 10\%$, the kink becomes more pronounced. For the highest strain amplitudes, the shear stress becomes independent of the strain amplitude for two quarters of a shear cycle. This indicates that shear thinning is occurring in the gel, producing a lozenge-shaped Lissajous figure. For higher deformations, the measured stress is strongly non sinusoidal and higher harmonics are clearly present in the waveform. The shear stress is independent of the strain over a large part of the cycle. It is important to note that the data collected in Fig. 3 were obtained sequentially, i.e. for the same sample the strain was increased incrementally. This could lead to shear history effects because even at $A = 10\%$ the flow is non-linear, thus the sample will be at least partially oriented, and this is the starting state for the higher strain amplitude measurements.

Lozenge-shaped Lissajous patterns at high amplitude strains have previously been observed for ordered micellar structures (Hamley et al. 1998b; Watanabe et al. 1982; Watanabe et al. 1997). Hamley et al. (1998) examined a 33 wt% gel of $E_{96}B_{10}$ forming a bcc phase via SAXS experiments on shear aligned gels. They reported that the non-ellipsoidal shape of the Lissajous figures at large strain amplitudes was associated with a macroscopic slip-stick mechanism of macroscopic alignment under large amplitude oscillatory shear (LAOS).

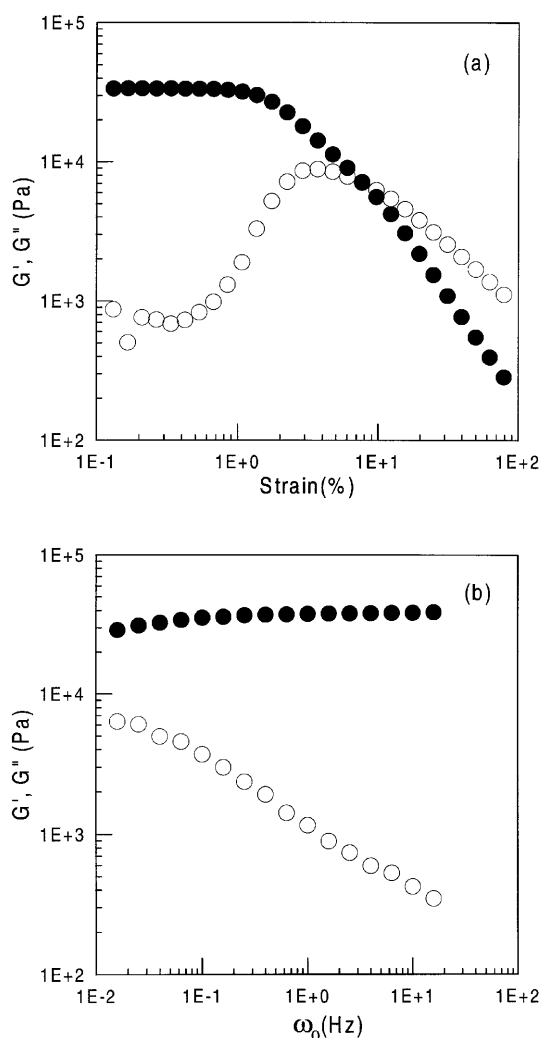


Fig. 2 (a) variation of the dynamic moduli G' (●) and G'' (○) versus strain at $\omega_0 = 1 \text{ Hz}$. (b) variation of the dynamic moduli G' (●) and G'' (○) versus frequency at a strain amplitude $A = 0.4\%$

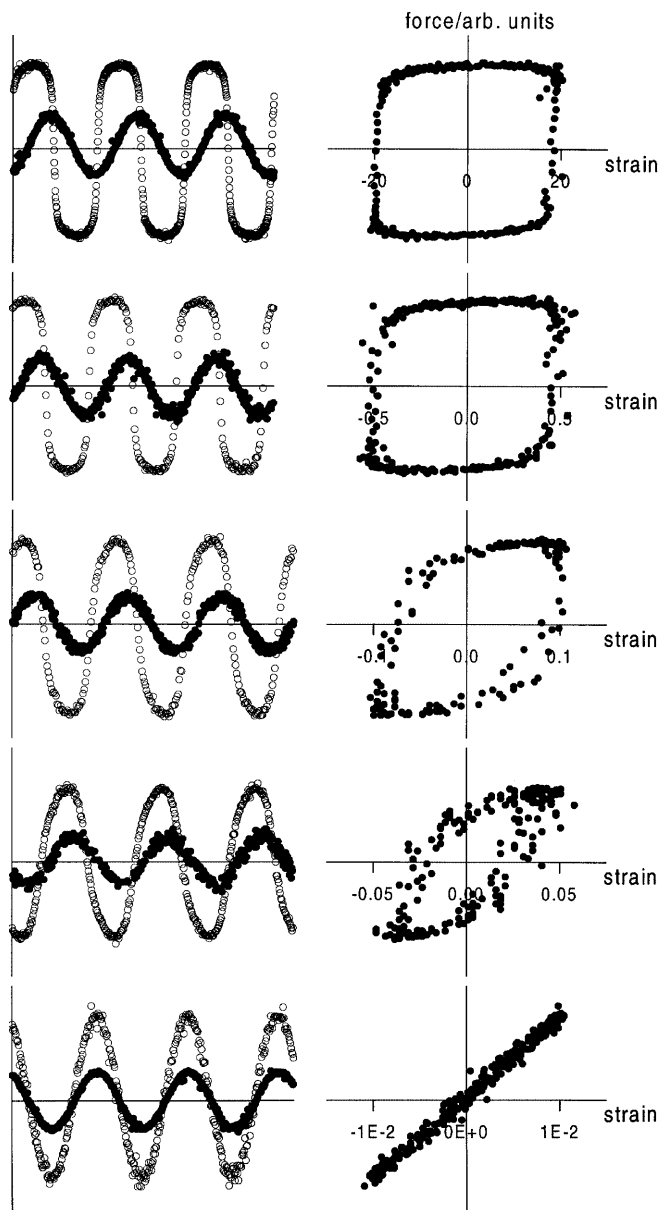


Fig. 3 Left: Rheometer output voltage corresponding to applied strain (●) and stress response (○) obtained under oscillatory deformation at $\omega_0 = 1$ Hz. The strain increases from bottom to top. The ordinates have been rescaled to give a common scale for strain or stress in each plot. Right: Lissajous patterns of the wave form data

This leads to permanent alignment of the bcc gel, as shown by experiments where the orientation has been monitored for up to one hour. There are important differences between the nonlinear flow of the fcc gel studied here and that for the bcc gel reported earlier (Hamley et al. 1998b). The bcc phase is more elastic than the fcc gel. This is manifested by the response at $A = 10\%$, for example. For the bcc gel, the strain and stress were in phase (Hamley et al. 1998b). In contrast,

Fig. 3 shows that in the fcc gel there is already a large phase shift, and that at the highest strain rate, the maximum stress occurs where the strain is near zero, i.e. at a maximum strain rate. This indicates that in the present fcc gel, pronounced shear thinning occurs at large strain amplitudes. On the other hand, in the bcc gel, a slip-stick mechanism was suggested to occur at large strain amplitudes, based on a sawtooth component in the stress response, i.e. a gradual build up of stress followed by release during part of a shear cycle. The origin of the differences in these mechanisms may simply be due to the difference in concentration (and/or shear frequency) or it may be due to the effect of microstructure on the flow mechanism. We consider first the former possibility. The more concentrated gel can be expected to exhibit a more elastic response. For the fcc system studied here we have not undertaken SAXS experiments on the 15 wt% gel under LAOS. However, we have examined in detail the effects of oscillatory (and steady) shear on a lower concentration (9 wt%) gel of the same copolymer, also forming an fcc phase (results from steady shear experiments have been published earlier (Hamley et al. 2000)). These results shed some insight into the flow mechanisms of an fcc micellar gel under LAOS. Figure 4 shows the 2D SAXS pattern obtained for the 9 wt% gel before shear (Fig. 4a) and under an oscillatory shear at $A = 1700\%$ and $\omega_0 = 0.2$ Hz (Fig. 4b). The partial orientation observed before shear is due to the sample loading. Upon application of LAOS, the structure was macroscopically aligned and the position of the reflections in the SAXS pattern indicate that the fcc structure became oriented with the $\{111\}$ planes parallel to the shear plane, indicating that slip occurs in $\{111\}$ planes (Hamley et al. 2000; Daniel et al. 2000). This is physically reasonable since they are the close-packed planes of an fcc structure. The same flow mechanism has previously been reported by others for charge- or sterically- stabilized colloids

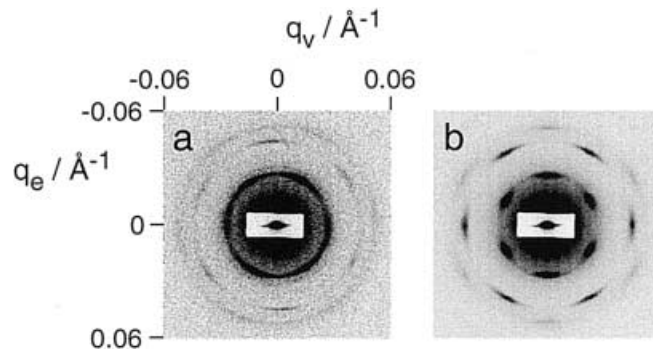


Fig. 4 SAXS patterns of an aqueous gel containing 9 wt% of $E_{96}B_{18}$ at 20 °C in the (q_v, q_e) plane where \mathbf{v} indicates the shear direction and $\mathbf{e} = \nabla \mathbf{v} \times \mathbf{v}$ the neutral (vorticity) direction. (a) sample as mounted, (b) during shear at $\omega_0 = 0.2$ Hz, $A = 1700\%$

(Ackerson and Pusey 1988; Ackerson 1990; Chen et al. 1994; Dux et al. 1996; Clarke et al. 1997), where it has been termed “layer sliding” (Ackerson 1990; Chen et al. 1994). The same alignment mechanism has also been observed for other block copolymer solutions (McConnell et al. 1995; Berret et al. 1996; Molino et al. 1998; Leyh et al. 1998).

Slip in the bcc phase also occurs in close-packed planes, being $\{110\}$ planes in this case (Ackerson and Clark 1984). However, the flow mechanism is quite distinct to that in the fcc phase. In the fcc phase, layer sliding occurs readily at sufficiently high shear rates as hexagonal close-packed layers slide over one another, destroying the ABCABC... stacking sequence of an fcc crystal. In the bcc phase, on the other hand, the bcc crystal structure is locally maintained for low shear rates, and slip is mediated by defects, specifically twinning planes (Ackerson and Clark 1984). At higher shear rates, however, flow can occur via a distorted two-dimensional hcp structure as layer sliding sets in (Ackerson and Clark 1984). The distinct flow behaviour of fcc and bcc crystals may reflect subtle differences in the intermicellar potential. The short-ranged potential between “hard spheres” in an fcc gel could favour layer sliding at moderate shear rates but hindered slip-stick motion in bcc gels where the potential is long-ranged. We note that the shear-induced orientation was retained upon cessation of shear for both fcc and bcc gels, so that relaxation effects cannot explain the difference in observed nonlinear flows.

In order to quantify the extent of the non-linear response of the gel when subjected to oscillatory strains at a frequency $\omega_0 = 1$ Hz, a Fourier analysis of the stress response was carried out. The meaning of the coefficients in the Fourier series expansion of the stress is discussed below in the context of Eq. (5). The Fourier spectra of the shear stress during oscillatory shear strain of different amplitudes are shown in Fig. 5. Values of the strain amplitude are $A = 1, 5, 10, 50, 100,$ and 2000% respectively. For a deformation of $A = 1\%$ the non-linear response of the gel is weak and only the third harmonic at $3\omega_0$ is detectable with a relative intensity of about $I(3\omega_0)/I(\omega_0) = 0.008$. Then, upon increasing the strain amplitude, the number of higher harmonics increases and for an applied strain of $A = 2000\%$ the frequency spectrum contains up to the 81st harmonic as detected by a single measurement where no further data averaging was performed. This result clearly shows the increase of the non-linear response of the structure with increasing strain amplitude.

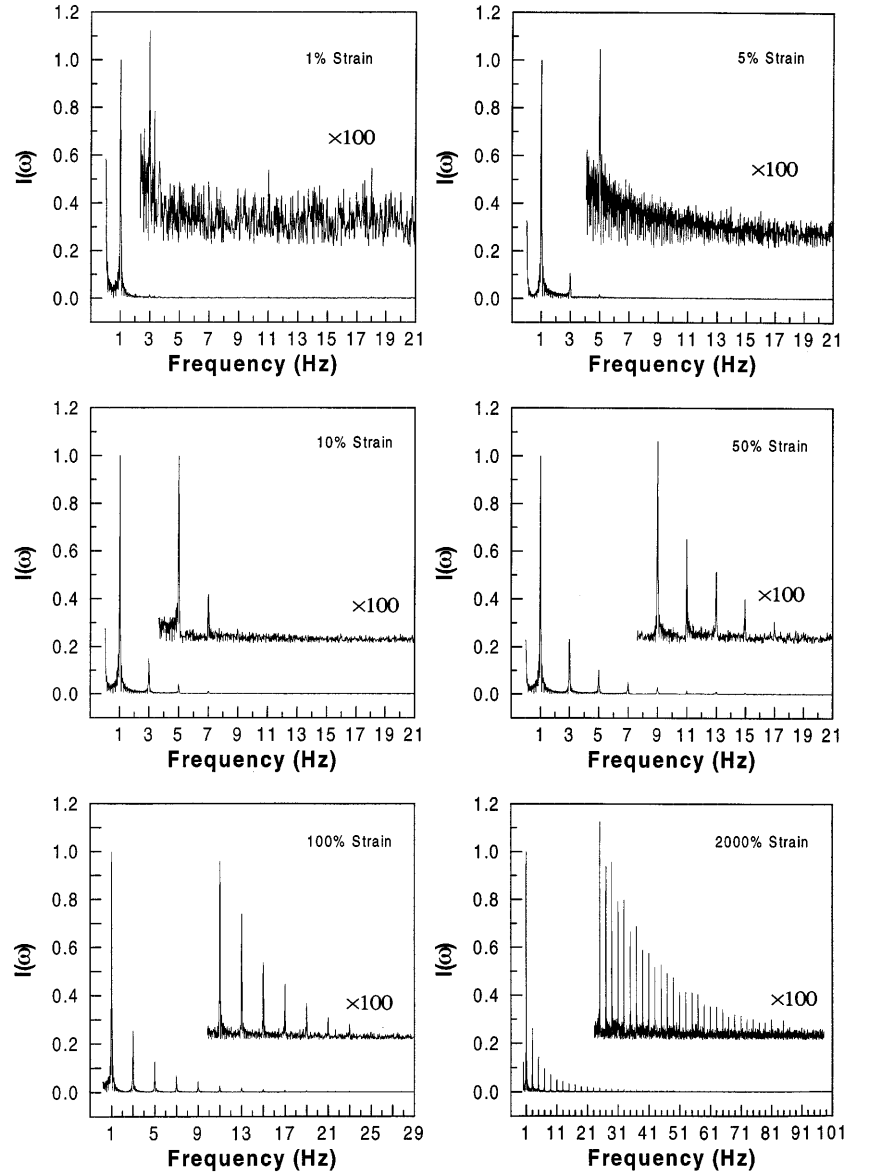
The variation of the amplitude of the third harmonic as a function of the strain amplitude is illustrated in Fig. 6. These plots are useful because the condition $I(3\omega_0) = 0$ can be used to define the linear regime. Up to approximately $A = 100\%$, $I(3\omega_0)/I(\omega_0)$ increases as

$\log(A)$ before an asymptotic value is reached. It is worth noticing that $I(5\omega_0)/I(\omega_0)$ and $I(7\omega_0)/I(\omega_0)$ also increase logarithmically up to $A = 100\%$ (not shown here). The intercept $I(3\omega_0)/I(\omega_0) = 0$ at a strain $A = 0.65\%$ suggests a cross-over between the linear and the non-linear regime. However, we note that with increased instrumental sensitivity it is possible that higher harmonics could be detected, i.e. that a linear regime would not strictly exist (Wilhelm et al. 2000). Nevertheless, the value $A = 0.65\%$ is in good agreement with the onset of the non-linear regime obtained from the variation of G' and G'' versus strain amplitude (cf. Fig. 2a). It can be observed that the progressive increase of G'' makes the determination of the cross-over between the linear and the non-linear regime much less accurate in a strain sweep measurement than in frequency space. It has been also reported previously that the presence of high harmonics is a more sensitive indicator of non-linearity than the variation of G' and G'' versus strain (Reimers and Dealy 1996).

An asymptotic behaviour for the amplitude of the harmonics has been predicted using a Carreau-type model, in the limit of extreme shear thinning that occurs for very large amplitude strains (Wilhelm et al. 1998). In this model the viscosity varies as $\eta/\eta_0 = 1/(1 + \beta\dot{\gamma}^\alpha)$, where α and β are constants. In the limit $\alpha = 1$, the oscillating stress becomes essentially independent of shear rate (i.e. $\eta \sim \dot{\gamma}^{-1}$) and can be described by a periodic step function. In this simplified model, the amplitude of the different harmonics at $n\omega_0$ decreases as $1/n\omega_0$ in the limit of large amplitudes. In our case, Lissajous patterns showed that for a strain amplitude $A = 2000\%$, the stress response is independent of the strain over a large period of the cycle (cf. Fig. 3). At this strain amplitude, the model predicts $I(3\omega_0)/I(\omega_0) = 1/3$ and $I(5\omega_0)/I(\omega_0) = 1/5$ but we observe $I(3\omega_0)/I(\omega_0) = 0.26$ and $I(5\omega_0)/I(\omega_0) = 0.14$. The decrease of the harmonic amplitudes is faster than the $1/n\omega_0$ variation predicted by the simple model of Wilhelm et al. 1998. This discrepancy is presumably due to the fact that the shear response cannot be accurately represented with a step function, i.e. α is less than unity. In fact, the rheometer output voltage reported in Fig. 3 shows the absence of sharp edges in the stress response. A possible additional contributing factor to reduced intensities for higher harmonics arises from memory related terms, which contribute differently when averaged over different time periods. A further limitation of the Carreau model is that it applies to steady flow behaviour, a state not attained in the LAOS measurements.

At sufficiently low frequencies, the behaviour of the micellar lattice, exhibiting plasticity, is determined by the strain. We thus present, in the next section, a model that accounts for the strain dependence of the stress response of a periodic (micellar) lattice.

Fig. 5 Fourier spectra of the rheometer stress response obtained with the aqueous gel containing 15 wt% E₉₆B₁₈ subjected to oscillatory deformation at $\omega_0 = 1$ Hz. The different applied strain amplitudes (bottom to top) are $A = 1, 5, 10, 50, 100,$ and 2000% . The amplitude of the fundamental frequency was normalized to $I(\omega_0) = 1$



Comparison to a model for the non-linear rheology

A lattice model based on connected Maxwell-Voigt cells was developed to describe the rheological response of surfactant cubic phases by Jones and McLeish (1995). It was assumed that the system can be described by a displacement variable $x_n(t)$, which in our case describes the position at time t of the n th layer of micelles from its unstrained position. At the current level of approximation, we consider only a two dimensional cross-section of layers as illustrated in Fig. 7, since the model is not expected to account for the distinct stress response of different planes in a cubic lattice, such as the face-centered cubic lattice considered here. In the following, we briefly outline the model

in order to introduce the equations used to model the non-linear stress harmonic coefficients. For a complete derivation, the reader is referred to Jones and McLeish (1995).

Considering one layer, displaced to x_n , a dissipative stress acting from the bulk below takes the form $\eta(\dot{x}_n - \dot{x}_{n-1})/a$, where η is the bulk viscosity and a is the lattice parameter. The corresponding elastic stress is $G(x_n - x_{n-1})/a$, where G is the bulk modulus. Balancing this stress with that from above leads to the following equation of motion

$$\frac{G}{a}(x_{n+1} - x_n) - \frac{G}{a}(x_n - x_{n-1}) + \frac{\eta}{a}(\dot{x}_{n+1} - \dot{x}_n) - \frac{\eta}{a}(\dot{x}_n - \dot{x}_{n-1}) = 0. \quad (1)$$

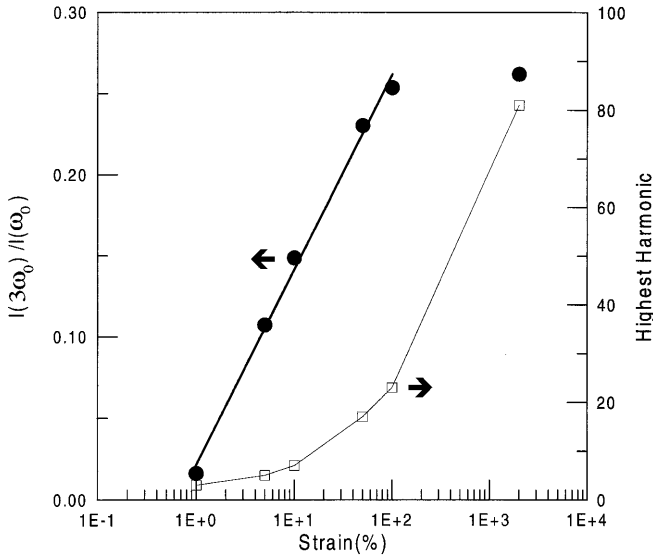


Fig. 6 Variation of $I(3\omega_0)/I(\omega_0)$ and highest harmonic observed as a function of applied shear strain amplitude

For small deformations, it is possible to take the continuum limit ($n \rightarrow s$) giving

$$\frac{\partial^2 x}{\partial s^2} = -\frac{\eta}{G} \frac{\partial^3 x}{\partial t^2 \partial s} . \quad (2)$$

It is thus possible to define a bulk relaxation time $\tau_i = \eta/G$ and solve this equation to obtain the following form

$$x(n, t) = aP(t)n + D(t) , \quad (3)$$

where $D(t)$ is zero if we impose the fixed boundary conditions $x(0, t) = 0$ and $x(N, t) = Na\gamma$, but will be non-zero if slip-planes are present (see below). In this case, $D(t)$ is related to the distance slipped. The quantity $P(t) = a^{-1} \partial x(n, t) / \partial n$ is the gradient of displacement in the bulk sample. For the no slip case this is equal to the strain $\gamma(t)$. The stress can now be computed as

$$\sigma = GP + \eta \dot{P} . \quad (4)$$

The first term is the elastic stress and the second is the viscous component. For the no slip case, $\sigma = G\gamma_0$, where G is a constant. Thus no stress relaxation occurs, and the system behaves as a solid at low frequencies, i.e. effectively as a Voigt cell. In order to model stress relaxation, Jones and McLeish (1995) allowed for slip planes. They derived analytical expressions for the dynamic shear moduli within theory for one slip plane linear response. However, the interest here is in the nonlinear response, which was also considered (Jones and McLeish 1995). If a sinusoidal strain $\gamma = \gamma_0 \sin \omega_0 t$ is applied to the system, the stress can be expanded as

$$\sigma(t) = \sum_{l=0}^{\infty} [G'(l)\gamma_0 \sin(l\omega_0 t) + G''(l)\gamma_0 \cos(l\omega_0 t)] \quad (5)$$

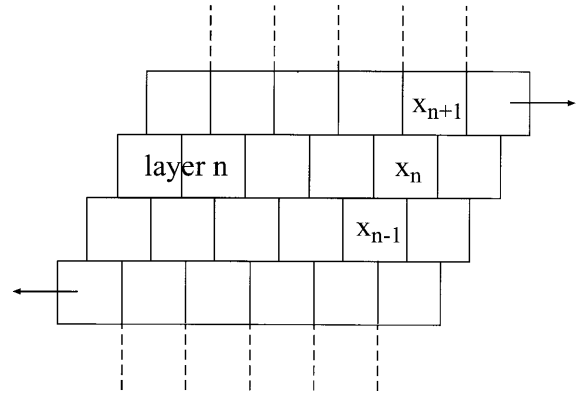


Fig. 7 Schematic of lattice Maxwell-Voigt model. A balance of forces act on a layer displaced to x_n when subjected to a sinusoidal strain. From above, there is an elastic stress $G \sin(2\pi(x_{n+1} - x_n)/a)$, and a viscous stress $\eta(\dot{x}_{n+1} - \dot{x}_n)/a$. From below there is an elastic stress $G \sin(2\pi(x_n - x_{n-1})/a)$, and a viscous stress $\eta(\dot{x}_n - \dot{x}_{n-1})/a$

where the terms $G'(l)$ and $G''(l)$ with $l \neq 0$ are non-zero in the non-linear regime and $G'(l=0)$ and $G''(l=0)$ are the usual storage and loss moduli respectively. The boundary condition at the slip plane allowing for a periodic lattice potential can be expressed as (Jones and McLeish 1995)

$$GP + \eta \dot{P} - \frac{\eta}{a} (\dot{x}_n - \dot{x}_{n-1}) - G_2 \sin(2\pi(x_n - x_{n-1})/a) = 0 \quad (6)$$

where G_2 is the elastic modulus at the slip plane due to the lattice potential. The non-linear response is analysed using a perturbation expansion, in which the gradient of the displacement, $P(t)$, is written as

$$P(t) = P_0(t) + \varepsilon P_1(t) + \varepsilon^2 P_2(t) + \dots , \quad (7)$$

with $G_2 = \varepsilon G$. Examination of the terms that are first order in ε in the perturbation expansion produces the following equation from the boundary condition

$$GP_1 + \eta \dot{P}_1 - G \sin\left(\frac{2\pi D}{a}\right) = 0 \quad (8)$$

The solution of this equation can be expressed in integral form using the Green function $P_1(t)$ and admitting only terms up to $P_0(t)$ in the source function. Evaluation of the integral eventually leads, following Jones and McLeish (1995), to the expression

$$P_1(t) = 2 \sum_{l=0}^{\infty} \frac{J_{2l+1}(\alpha)}{1 + \omega_0^2 \tau^2 (2l+1)^2} [\sin((2l+1)(\phi + \omega_0 t)) - \omega_0 \tau (2l+1) \cos((2l+1)(\phi + \omega_0 t))] . \quad (9)$$

Here J_{2l+1} denotes a Bessel function of argument $\alpha = 2\pi N \gamma_0 ((1 + (r_n \omega_0 \tau / (r_n + N))^2) / (1 + \omega_0^2 \tau^2))^{1/2}$ and $\tan \phi = (1 + \omega_0^2 \tau \tau_1) / \omega_0 (\tau - \tau_1)$. The relaxation time τ is that for a single slip plane. In the expression for α ,

$r_\eta = \eta/\eta_2$ is the ratio of the bulk viscosity to the slip plane viscosity. Finally, we obtain the stress via Eq.(4) (Jones and McLeish 1995).

We attempted to use Eq. (9) with Eq. (4) to fit the harmonics shown in Fig. 5 (taking the absolute value of σ). The following procedure was adopted to reduce the number of fit parameters: The frequency of applied strain $\omega_0 = 1$ Hz was fixed, as was $G \sim G'(\omega_0 = 1 \text{ Hz}) = 3 \times 10^4$ Pa and the strain amplitude (values as in Fig. 5). This left η , η_2 and N as fit parameters. Fourier coefficients up to $l=5$ were included. Unfortunately it proved not to be possible to fit the data within this model. However it was possible to reproduce qualitative trends, i.e. (i) decreasing amplitude of successively higher harmonics at fixed strain and (ii) amplitude of a given harmonic increasing with strain. Representative values are given in Table 1.

Summary

We have studied the non-linear response of an fcc micellar structure formed by a diblock copolymer in aqueous solution subjected to LAOS. Upon increasing strain, the stress response was found to be strongly non-linear and strong shear thinning was indicated from the shape of Lissajous patterns of stress as a function of strain. SAXS experiments showed that under LAOS, slip of the fcc gel occurred in $\{111\}$ planes. The non-linear response of the gel was then further investigated using a Fourier transform analysis. We observed that the high harmonic contributions increase with increasing strain and up to the 81st harmonic was observed for a strain amplitude of

Table 1 Measured and fitted harmonic amplitudes (relative to $l = 0$) corresponding to the data in Fig. 5

$\omega/\text{Hz} (2l+1)$	$\gamma = 1\%a$		$\gamma = 100\%b$	
	Measured	Fit	Measured	Fit
1	1	1	1	1
3	0.016	0.016	0.253	0.266
5	0	0	0.126	0.017
7	0	0	0.069	0.005
9	0	0	0.045	7.6×10^{-5}
11	0	0	0.027	8.0×10^{-7}

^a Fit coefficients: $\eta = 57$ Pa s, $N = 133$, $r_\eta = 0.019$;

^b Fit coefficients: $\eta = 1 \times 10^4$ Pa s, $N = 1008$, $r_\eta = 0.107$

2000%. The analysis in the Fourier space allowed us to determine with precision the onset of the non-linear regime. It was also found that the amplitude of the harmonics $I(3\omega_0)$, $I(5\omega_0)$, and $I(7\omega_0)$ increases logarithmically with strain amplitude up to $A = 100\%$ before reaching an asymptotic value. A Maxwell-Voigt model for the non-linear stress assuming a weakly periodic lattice potential in slip planes was unable to model this behaviour quantitatively, but was able to reproduce observed trends of monotonically decreasing harmonic coefficients at a fixed strain and increase in harmonic intensities with strain.

Acknowledgements CD and DvD were supported as postdoctoral fellows within the EU-TMR network ‘‘Complex Architectures in Diblock Based Copolymer Systems’’. Beamtime at Daresbury was provided under EPSRC grant GR/L79854 to IWH. WM thanks the Thai government for support. We are grateful to Colin Booth (University of Manchester) for comments on a draft of this manuscript.

References

- Ackerson BJ (1990) Shear Induced Order and Shear Processing of Model Hard Sphere Suspensions. *J. Rheol.* 34:553
- Ackerson BJ, Clark NA (1984) Shear-Induced Partial Translational Ordering of a Colloidal Solid. *Phys. Rev. A* 30:906
- Ackerson BJ, Pusey PN (1988) Shear-Induced Order in Suspensions of Hard Spheres. *Phys. Rev. Lett.* 61:1033
- Almgren M, Brown W, Hvidt S (1995) Self-aggregation and Phase Behavior of Poly(ethyleneoxide)-Poly(propylene oxide)-Poly(ethylene oxide) Block Copolymers in Aqueous Solution. *Colloid Polym. Sci.* 273:2
- Berret J-F, Molino F, Porte G, Diat O, Lindner P (1996) Shear-Induced Transition Between Oriented Textures and Layer Sliding Mediated Flows in a Micellar Cubic Crystal. *J. Phys. – Condens. Matt.* 8:9513
- Chen LB, Ackerson BJ, Zukoski CF (1994) Rheological consequences of Microstructural Transitions in Colloidal Crystals. *J. Rheol.* 38:193
- Clarke SM, Rennie AR, Ottewill RH (1997) Stacking of Hexagonal Layers of Colloidal Particles: Study by Small-Angle Neutron Diffraction. *Langmuir* 13:1964
- Daniel C, Hamley IW, Mingvanish W, Booth C (2000) Effect of Shear on the Face-Centered Cubic Phase in a Diblock Copolymer Gel. *Macromolecules* 33:2163
- Doi M, Harden JL, Ohta T (1993) Anomalous Rheological Behaviour of Ordered Phases of Block Copolymers. *Macromolecules* 26:4935
- Dux C, Vermold H, Reus V, Zemb T, Lindner P (1996) Neutron Diffraction from Shear Ordered Colloidal Dispersions. *J. Chem. Phys.* 104:6369
- Gamota RD, Wineman AS, Filisko FE (1993) Fourier Transform Analysis: Nonlinear Dynamic Response of an Electrorheological Material. *J. Rheol.* 37:919
- Hamley IW (1998) Block Copolymers in Semidilute and Concentrated Solutions. Chapter 4, *The Physics of Block Copolymers* (Oxford University Press, Oxford)
- Hamley IW (2000) Amphiphilic Diblock Copolymer Gels: The Relationship between Structure and Rheology. *Phil. Trans. R. Soc. Lond.*, in press
- Hamley IW, Pople JA, Fairclough JPA, Terrill NJ, Ryan AJ, Booth C, Yu G-E, Diat O, Almdal K, Mortensen K, Vigild M (1998a) Effect of Shear on Cubic Phases in Gels of a Diblock copolymers. *J. Chem. Phys.* 108:6929
- Hamley IW, Pople JA, Booth C, Derici L, Imp rator-Clerc M, Davidson P (1998b)

- Shear Induced Orientation of the Body-centered-cubic Phase in a Diblock Copolymer Gel. *Phys. Rev.* 58:7620
- Hamley IW, Daniel C, Mingvanish W, Mai S-M, Booth C, Messe L, Ryan AJ (2000) From Hard Spheres to Soft Spheres: The Effect of Corona Block Length on the Structure of Micellar Cubic Phases formed by Diblock Copolymers in Aqueous Solution. *Langmuir* 16:2508
- Hvidt S, Jørgensen EB, Brown W, Schillén K (1994) Micellization and Gelation of Aqueous Solutions of a Triblock Copolymer Studied by Rheological Techniques and Scanning Calorimetry. *J. Phys. Chem.* 98:12320
- Jones JL, McLeish TCB (1995) Rheological Response of Surfactant Cubic Phases. *Langmuir* 11:785
- Leyh B, Creutz S, Gaspard J-P, Bourgaux C, Jérôme R (1998) Shear-induced order in aqueous micellar solutions of amphiphilic poly(*tert*-butylstyrene)-*b*-poly(Na methacrylate) diblock. *Macromolecules* 31:9258
- McConnell GA, Lin MY, Gast AP (1995) Long Range Order in Polymeric Micelles under Steady Shear. *Macromolecules* 28:6754
- Mingvanish W, Mai S-M, Heatley F, Booth C, Attwood D (2000) Association Properties of Diblock Copolymers of Ethylene Oxide and 1,2-Butylene Oxide in Aqueous Solution. Copolymers with Oxyethylene-Block Lengths in the Range 100–400 Chain Units. *J. Phys. Chem. B*, in press.
- Molino F R, Berret J-F, Porte G, Diat O, Lindner P (1998) Identification of Flow Mechanisms for a Soft Crystal. *Eur. Phys. J. B* 3:59
- Mortensen K (1992) Phase Behaviour of Poly(ethylene oxide)-Poly(propylene oxide)-Poly(ethylene oxide) Triblock-Copolymer Dissolved in Water. *Europhys. Lett.* 19:599
- Mortensen K, Brown W, Nordén B (1992) Inverse Melting Transitions and Evidence of Three-dimensional Cubatic Structure in a Block-copolymer Micellar System. *Phys. Rev. Lett.* 68:2340
- Pople JA, Hamley IW, Fairclough JPA, Ryan AJ, Komanschek BU, Gleeson AJ, Yu G-E, Booth C (1997) Ordered Phases in Aqueous Solutions of Diblock Oxyethylene/Oxybutylene Copolymers Investigated by Simultaneous Small-angle X-ray Scattering and Rheology. *Macromolecules* 30:5721
- Pople JA, Hamley IW, Fairclough JPA, Ryan AJ, Hill G, Price C (1999) A Shear-Induced Transition of Lamellar Alignment in a Concentrated Diblock Copolymer Solution. *Polymer* 40:5709
- Reimers MJ, Dealy JM (1996) Sliding Plate Rheometer Studies of Concentrated Polystyrene Solutions: Large Amplitude Oscillatory Shear of a Very High Molecular Weight Polymer in Diethyl Phthalate. *J. Rheol.* 40:167.
- Reimers MJ, Dealy JM (1998) Sliding Plate Rheometer Studies of Concentrated Polystyrene Solutions: Nonlinear Viscoelasticity and Wall Slip of Two High Molecular Weight Polymers in Tricresyl Phosphate. *J. Rheol.* 42:527
- Watanabe H, Kotaka T, Hashimoto T, Shibayama M, Kawai H (1982) Rheological and Morphological Behavior of Styrene-Butadiene Diblock Copolymer Solutions in Selective Solvents. *J. Rheol.* 26:153
- Watanabe H, Sato T, Osaki K, Yao M-L, Yamagishi A (1997) Rheological and Dielectric Behavior of a Styrene-Isoprene-Styrene Triblock Copolymer in Selective Solvents. 2. Contribution of Loop-type Middle Blocks to Elasticity and Plasticity. *Macromolecules* 30:5877
- Wilhelm M, Maring D, Spiess H-W (1998) Fourier-Transform Rheology. *Rheol. Acta* 37:399
- Wilhelm M, Reinheimer P, Ortseifer M (1999) High Sensitivity Fourier-Transform Rheology. *Rheol. Acta* 38:349
- Wilhelm M, Ortseifer M, Neidhoefer T, Spiess H-W (2000) The Crossover Between Linear and Non-linear Behaviour in Polymer Solution as Detected by Fourier-Transform Rheology. *Rheol. Acta*, in press.
- Yu G-E, Li H, Fairclough JPA, Ryan AJ, McKeown N, Ali-Adab Z, Price C Booth C (1998) A Study of Lyotropic Mesophases of Concentrated Solutions of a Triblock Copolymer of Ethylene Oxide and 1,2-Butylene Oxide, E₁₆B₁₀E₁₆, Using Rheometry, Polarized Light Microscopy and Small-Angle X-ray Scattering. *Langmuir* 14:5782